Chapter 8

Conclusions and Future Work

8.1 Summary and Conclusions

The thesis comprises of two parts, Part I - Modern Oceanography and Part II - Oceanographic change over the late Quaternary. The main aim of the thesis was to understand spatial and temporal variations in intermediate waters of the south Pacific, and correlation of these variations with ocean circulation and climate change.

The main conclusions from Part I are the presence of three intermediate water masses in the Pacific Ocean. North Pacific Intermediate Water (NPIW) from the north Pacific, the Antarctic Intermediate Water (AAIW) in the south Pacific, and Equatorial Intermediate Water (EqIW) in the tropics. EqIW should be considered an independent water mass as a result of its distinct geochemical properties which are formed from a combination of mixing between the NPIW and AAIW and upwelling nutrient rich, oxygen deficient, old Pacific Deep Waters (PDW).

The AAIW is primarily formed and sourced from the southeast Pacific along with the Subantarctic Mode Water (SAMW). However, variations in the physical properties and geochemical characteristics of the AAIW are formed as a result of isopycnal mixing along its path around the subtropical gyre. Two other main mixing sources are implicated from the geochemical characteristics. A second source and significant mixing occur in the eastern equatorial Pacific (EEP) as a result of mixing with the EqIW. A third, minor source, enters the south Tasman Sea.

Circulation of the AAIW follows the main subtropical gyre surface circulation with an exit south along the Tonga-Kermadec Ridge and another southward flow adjacent to the South American coast. This second exit appears to be made up of a combination of AAIW and an overlying tongue of EqIW flowing south from the tropics. Within the Tasman Sea and Coral Sea, the AAIW is relatively uniform, but distinct from the AAIW in the main subtropical gyre. This suggests that there is a separate recirculating gyre in this region. These studies and understanding the present day $\delta^{13}C$ distribution in the intermediate waters is critical for the use of foraminiferal carbon isotopes as an ocean circulation tracer

in the past.

In Part II, a series of marine sediment cores. The cores comprise a depth transect extending from 166 mbsl to ∼3000 mbsl from the Capricorn Channel, southern Great Barrier Reef (GBR) province. Data from these cores have provided a preliminary picture of the hemipelagic sedimentation of the region over the last glacial/interglacial cycle. The sedimentary variation within the cores is primarily related to sea level fluctuations but differs from the sedimentary models produced for the northern GBR province as a result of the different morphology and bathymetry of the adjacent reef platforms and continental shelf.

Core FK1/97 GC-12, extracted from intermediate waters, exhibits a high sedimentation rate from which it is possible to study changes in the AAIW through during the last glacial/interglacial transition. A suite of planktonic foraminifera and benthic foraminifera were used for stable isotope analyses to highlight changes in the water column over the last deglaciation. Rapid variations in the $\delta^{13}C$ of the foraminifera and the $\Delta\delta^{13}C$planktonic-benthic offset are evident during the last glacial/interglacial transition, Termination I. The $\Delta\delta^{13}C$planktonic-benthic offset decreases to 0.4‰ compared to 1.1‰ during the glacial and 0.7‰ during the Holocene and present. The reason for this significant decrease in the $\Delta\delta^{13}C$planktonic-benthic offset at the deglaciation is suggested to be the result of a rapid ventilation of the AAIW in the south Pacific. During this ventilation the AAIW is implicated as the driver for the release of deep-water CO_2 resulting in a coeval rapid rise in atmospheric CO_2. In the Tasman Sea, it is hypothesised that the southern source of the AAIW possibly increased in dominance during the glacial. The switch back to a dominantly northeastern AAIW source in the Coral Sea coincides with the ventilation event and the re-initiation of the present subtropical gyre circulation. It is evident from the three phases of carbon isotope changes that the carbon cycle and the distribution of carbon between the atmosphere, surface water and subsurface intermediate water reservoirs varies considerably on a glacial/interglacial timescale.

The final Chapter turns its attention to variations in the circulation of the East Australian Current (EAC), the western boundary current (WBC) of the south Pacific. Surface currents in the oceans are primarily driven by the wind stress field. Recent models suggest that the modern EAC separation and the formation of the Tasman Front at ∼ 26°S are related to the wind stress curl τ of the south Pacific. Using two high sedimentation rate cores from the continental slope of the east Australian coast, GC-12 from the Capricorn Channel (sim23°S) and GC-25, (∼26°S), oxygen isotope evidence is provided to suggest that the EAC separation shifted north of ∼26° during the glacial. The palaeo-evidence suggests that the tropical trade winds were reduced as a result of a reduced east-west SST gradient, while the subtropical westerlies shifted north and increased in strength. These changes potentially altered the wind stress field and consequently the wind stress curl, resulting in a more northerly separation of the EAC from east Australian.

The cores show a rapid convergence of the $\delta^{18}O$ data between 12-11 ka BP. This suggests that the separation of the EAC shifted south of ∼26°S. This is the initiation of

present day circulation in the south Pacific and correlates with evidence of rapid warming of tropical SSTs and subsequent enhancement of the trade winds. The timing of this shift in the EAC separation at ∼12-11 ka BP is similar to the timing of the transition to Phase 3 of the carbon isotopes noted in chapter 6. This is unlikely to be coincidental and it is probably related to a major shift in global atmospheric and oceanic circulation at this time. A further convergence of the $\delta^{18}O$ *G. ruber* data from GC-12 and GC-25 occurred after ∼5 ka BP when present modern conditions are fully restored.

In this thesis the use of geochemical tracers, especially stable and radioactive isotopes of oxygen and carbon, has helped to elucidate the modern distribution, sources and circulation of the intermediate waters in the Pacific, particularly on the EqIW and the AAIW. This knowledge of the modern isotope distribution is used to interpret the palaeoceanography of the AAIW and EAC in the Tasman Sea and Coral Sea in the southwest Pacific.

8.2 Future Work

The south Pacific is an understudied region of the global oceans and therefore this is essentially a preliminary study of the geochemistry of the intermediate waters. More work on the present oceanography and palaeoceanography is essential for a more detailed understanding of this region.

It is evident that the south Pacific, and specifically the AAIW, plays an important role in ocean circulation and climate change and therefore an understanding of its formation mechanisms, sources and distribution will hopefully aid future predictions by climate models. A cruise to the southeast Pacific is being undertaken in early 2005 specifically to study the AAIW and SAMW formation (Talley, pers comm.)

In the past not many cores have been studied to look specifically at variations in the palaeoceanography of the AAIW. A broad distribution of high resolution sedimentary cores from around the south Pacific region would aid the interpretation of the AAIW distribution and geochemical properties during the LGM and deglaciation. This work has been started, specifically in the southeast Pacific (Ninneman, pers comm.) The use of additional tracers (e.g. Cd/Ca) for the AAIW water mass, used in combination with $\delta^{13}C$, would be useful to determine between the different factors affecting the carbon isotopes and help with the interpretation of ocean circulation changes.

The EAC is an important current for the east Australian coast, and understanding its variations as a result of El Niño or other climate/oceanography oscillations will help the forecasting of droughts and weather conditions on the Australian continent. Detailed changes of seasonal variations over hundreds of years are available from long living *Porites* coral $\delta^{18}O$ records, but an understanding of how ENSO has varied in frequency and long term changes will require more high resolution cores from the Coral Sea and Tasman Sea. $Mg:Ca$ measured on the skeletal carbonate of foraminifera is also becoming a common technique which will help separate the $\delta^{18}O$ changes caused by temperature and salinity. This will help in the determination of changes over time in the surface currents and oceanic

fronts.

A further understanding of hemipelagic sedimentation may help with the targeting of suitable depths and areas to obtain high sedimentation rate cores. High resolution sedimentary records are essential to understand these detailed palaeoceanographic changes through time, allowing the oceanic records from the tropics, subtropics and temperate regions to be correlated with the high latitude, high resolution, ice core records. This will help to further understand the possible mechanisms involved in global climate change, including the precessional insolation driven tropical forcing. However, this also requires improvements in accurate chronologies of different palaeo-data sets to allow for meaningful correlations.

Further study of the carbon species distributions in the present and past oceans is still required to accurately model the carbon cycle and understand its influence and feedbacks on global climate change in the present and past.

Appendix A

Studying the Carbonate System

There are four main parameters of the carbonate system that are commonly measured, pH, alkalinity, TIC and fugacity of CO_2. From a combination of at least two of these the whole system can be characterised (*Park*, 1969). The main problem with the different parameters is how accurate they can be measured at source. This leads to errors when calculating the other parameters within the system (*Millero et al.*, 1993).

A.1 Alkalinity

Alkalinity is defined as all the bases that can accept a proton at the carbonic acid end point (*Dickson*, 1981). Alkalinity varies more or less directly with salinity and is sometimes expressed as specific alkalinity (*Butler*, 1982). The normal range for surface water alkalinity is 2.3-2.6 mmole/kg.

$$\begin{aligned} TotalAlk &= [HCO_3^-] + 2[CO_3^{2-}] + [B(OH)_4^-] + [OH^-] - [H^+] + [SiO(OH)_3^-] + \\ &\quad [HPO_4^{2-}] + 2[PO_4^{3-}] + [HS^-] + 2[S^{2-}] + [NH_3] - [HSO_4^-] - \\ &\quad [HF] - [H_3PO_4] \end{aligned}$$

However only the Alkalinity due to CO_2 is required - the Carbonate Alkalinity - CA which is defined as:

$$CA = [HCO_3^-] + 2[CO_3^{2-}]$$

To calculate CA from Total Alkalinity we must account for the contributions from the other ions, especially $[B(OH)_4^-]$, $[OH^-]$, $[H^+]$. Where $[B(OH)_4^-]$ is determined to contribute almost 3% at a pH of 8 (*Butler*, 1982). Although the majority of workers do not correct for this.

A.2 TIC - Total Inorganic Carbon

Total Inorganic Carbonate (TIC) or ΣCO_2 is defined as:

$$TIC = [CO_2\star] + [HCO_3^-] + [CO_3^{2-}]$$

Carbonate production, therefore, consumes alkalinity and TIC in a ration of 2:1. Hence TIC is always less than alkalinity. Average TIC for surface ocean water is 2 - 2.2 μmole/kg.

At any one time, in a closed system, TIC is constant. With varying pH different concentrations of carbon ions can be found as a result of the buffering effect of the carbonate system as shown by the equations below.

ΣCO_2 in solution is thermodynamically controlled by:

$$\begin{aligned} CO_2(g) &\overset{K_0}{\rightleftharpoons} CO_2(aq) \\ CO_2(aq) + H_2O &\overset{K_H}{\rightleftharpoons} H_2CO_3 \\ CO_2 + H_2O &\overset{K_1}{\rightleftharpoons} H^+ + HCO_3^- \\ HCO_3^- &\overset{K_2}{\rightleftharpoons} H^+ + CO_3^{2-} \end{aligned}$$

K_0 - Solubility Constant (Henry's Law constant)
K_H - Hydration Constant
K_1 - 1st Dissociation Constant of Carbonic Acid
K_2 - 2nd Dissociation Constant of Carbonic Acid

$K_H \approx 10^{-3}$ - so most of the undissociated dissolved CO_2 is in the form of CO_2 (aq), therefore CO_2 (aq) and H_2CO_3 are usually just considered the same species and written as $CO_2^\star$.

$$\begin{aligned} lnK_0 = &-60.2409 + 93.4517(\frac{100}{T}) + 23.3585ln(\frac{T}{100}) + \\ &S(0.023517 - 0.023656(\frac{T}{100}) + 0.0047036(\frac{T}{100})^2) \end{aligned}$$

Where T is temperature in Kelvin, S is salinity in ‰, and the answer is expressed in moles kg^{-1} atm^{-1} (*Weiss*, 1974)

$$\begin{aligned} K_1 &= \frac{[H^+][HCO_3^-]}{[CO_2^\star]} \\ K_2 &= \frac{[H+][CO_3^{2-}]}{[HCO_3^-]} \end{aligned}$$

$$\begin{aligned} pK_1 &= \frac{3633.86}{T} - 61.2172 + 9.67770lnT - 0.011555S + 0.0001152S^2 \\ pK_2 &= \frac{471.78}{T} + 25.9290 - 3.16967lnT - 0.01781S + 0.0001122S^2 \end{aligned}$$

(*Lueker et al.* (2000) - derived from *Mehrbach et al.* (1973).

Many different studies have been undertaken using a range of different values and equations for K_1 and K_2 including *Mehrbach et al.* (1973), *Hansson* (1973), *Dickson and Millero* (1987), *Goyet and Poisson* (1989), *Roy et al.* (1993). The accuracies, adjustments and problems of these thermodynamic constants for K_1 and K_2, determined by the different workers, are discussed by *Millero* (1995).

A.3 pH

$$pH = -log[H^+]$$

pH is affected by changes in temperature and these have to be corrected for as the measurements are not taken in situ. Average surface ocean pH ranges from 7.8 - 8.4.

$$pHsws = 8.210 - 1.582 * 10^{-2}t$$

Where t is 25 °C.

To determine it for temperatures further away from 25°C

$$\begin{aligned} pHt &= pH_{25} + (-2.6492 - 0.0011019S + 4.9319 * 10^{-6}S^2 + \\ &\quad 5.1872(\frac{Alk}{TIC}) - 2.1586(\frac{Alk}{TIC})^2) + \\ &\quad (0.10265 - 0.20322(\frac{Alk}{TIC}) + 0.084431(\frac{Alk}{TIC})^2 + \\ &\quad 3.1618 * 10^{-5}S)t + (4.4528 * 10^{-5})t^2 \end{aligned}$$

For values of pHsws from 0-40°C, S = 30-40 ‰ and pH from 7.5-8.5. Where standard error of pH is 0.003. (*Millero*, 1995)

A.4 Fugacity of CO_2

Fugacity of CO_2 or the partial pressure of CO_2 (pCO_2) is defined as:

$$fCO_2 = \frac{[CO2\star]}{K_0} \tag{A.1}$$

Average fCO_2 (pCO_2) for surface waters is 0.25 - 0.45 10^{-3} atm.

Fugacity is the measure of the tendency of a gas to escape or expand. It is the pressure value needed at a given temperature to make the properties of a non-ideal gas satisfy the equation for an ideal gas $f_i = \gamma_i P_i$ where γ_i is the fugacity coefficient and P_i is the partial pressure for the component i of the gas. For an ideal gas $\gamma_i = 1$. Where f_i becomes equal to P_i at low pressures.

A.5 Carbonate Saturation - Calculating the Lysocline

The solubility and precipitation of $CaCO_3$ as aragonite and calcite also affect both alkalinity and TIC.

$$\begin{aligned} CaCO_3(s) &\rightleftharpoons Ca^{2+} + CO_3^{2-} \\ K_{SP} &= [Ca^{2+}][CO_3^{2-}] \end{aligned}$$

Where K_{SP} is the solubility product.

The solubility of $CaCO_3$ in seawater is:

$$\begin{aligned} LogK_{calcite} &= -171.9065 - 0.077993T + \frac{2839.319}{T} + 71.595logT + \\ &\quad (-0.77712 + 0.0028426T + \frac{178.34}{T}) \\ &\quad S^{0.5} - 0.07711S + 0.0041249S^{1.5} \\ LogK_{aragonite} &= -171.945 - 0.077993T + \frac{2903.293}{T} + 71.595logT + \\ &\quad (-0.068393 + 0.0017276T + \frac{88.135}{T}) \\ &\quad S^{0.5} - 0.10018S + 0.0059415S^{1.5} \end{aligned}$$

where T is temperature in Kelvin, S is salinity in ‰ (*Mucci*, 1983). These can be used to calculate the saturation states of calcite and aragonite using:

$$\begin{aligned} \Omega_{calcite} &= \frac{[Ca^{2+}][CO_3^{2-}]}{K_{calcite}} \\ \Omega_{aragonite} &= \frac{[Ca^{2+}][CO_3^{2-}]}{K_{aragonite}} \end{aligned}$$

where $[Ca^{2+}]$ is fairly constant throughout seawater at (*Millero*, 1982):

$$[Ca^{2+}] = 0.01028(\frac{S}{35})$$

Saturation states are used to determine the lysocline of the deep oceans. When $\Omega = 1$ the seawater is saturated with respect to carbonate. This is the situation in the surface oceans. However, with decreasing temperature and increasing pressure, (the latter is more important), carbonate is more soluble and the surrounding water becomes increasingly undersaturated. Two separate equations for the different morphologies of the carbonate are used as aragonite is less stable. Hence, the lysocline for aragonite is shallower than that for calcite.

The CO2SYS software, a DOS program, was used to calculate the different parameters and concentrations of the ions within the CO_2 marine carbonate system using the TIC and alkalinity, temperature, salinity and depth. This program (version 01.04) written by Ernie Lewis, Oceanographic and Atmospheric Science Division, Brookhaven National Laboratory. It was developed as part of the 'Inorganic carbon for the World Ocean Circulation Experiment - World Hydrographic Program.

Appendix B

Radiocarbon Analyses and Corrections

The Accelerator Mass Spectrometry (AMS) Unit is housed at the Research School of Physical Sciences and Engineering (Nuclear Physics), The Australian National University.

The majority of ^{14}C dates that have used the "conventional methods" involving the measurement of electrons being emitted by radioactive decay. Such methods require samples of 1-5 g of carbon and takes several days to measure. AMS is now more commonly used as it requires smaller samples (0.5-2 mg of carbon in the form of graphite). AMS uses high energy mass spectrometer systems to measure the ^{14}C isotope by ion counting and takes less than an hour to determine rather than days.

AMS (the radiocarbon dating practices at ANU 1985) Tandem accelerators require negative ions. To generate the required negative carbon ion beam (C^-) from the target holding the sample, a cesium (Cs^+) ion source is always used. The source is very versatile and can produce C^- ions from almost any carbon bearing solid and CO_2 gas. However results have shown that it is better to use solid sources as gas ion sources have been found to show large memory effects. Significant sample preparation is required to convert some samples into a graphite target.

$CaCO_3$ in the form of shells, coral, soils, caliche or dissolved ions in water such as HCO_3^-, CO_2(aq) etc. must undergo initial hydrolysis to CO_2(g). The CO_2(g) is then reduced at high temperatures to a mixture of elemental carbon (graphite) in the presence of hydrogen and iron catalyst. The graphite is pressed into a cathode and measured on the AMS.

The AMS results are reported as Percent Modern Carbon (PMC) where:

$$PMC_{std} = 150.8\%$$

where the std = standard, which is normalised to a $\delta^{13}C$ = -25‰. The actual standard used is the ANU sucrose, which displays a $\delta^{13}C$ = -10.8‰.

$$PMC^m_{smpl} = \left((\frac{^{14}C}{^{13}C})^m_{smpl} / (\frac{^{14}C}{^{13}C})^m_{std} \right) * 150.8$$

where smpl = sample and m = measured. The true PMC requires a normalisation of the real $\delta^{13}C$ of the standard and sample.

$$TruePMC = PMC^{m}_{smpl} * \left(\frac{1 - \delta^{13}C_{smpl}/1000}{1 - \delta^{13}C_{std}/1000} \right)$$

For marine samples the $\delta^{13}C = \sim 1‰$.

To work out the conventional radiocarbon age;

$$t = -8033 ln \left(\frac{TruePMC}{100} \right)$$

Where t = radiocarbon age based on a half life of 5568 years.

The conventional radiocarbon age requires calibration to calendar years in order to compare with other global records. This calibration can be done using several programs which use standard databases such as INTCAL98 and MARINE98 (*Stuiver et al.*, 1998). These databases presently provide a good calibration back to 20,000 years and correct for the real radiocarbon half life of 5730 years and allow a localised reservoir correction value to be used. This local reservoir correction is a constant, although it may have changed considerably through time. New databases are presently being compiled to extend the calibration age range back to 24,000 years (*Bard et al.*, 2004).

Beyond 20,000 years the polynomial of *Bard et al.* (1998) is used, which utilises coupled U/Th dates with radiocarbon dates in corals from Barbados, Tahiti and Mururoa. Samples of 200 years or younger are reported as *Modern* due to the complications of the bomb and Suess effects.

For Heron Island, southern Great Barrier Reef, the reservoir correction is ΔR of 8±7 with a reservoir age of 344±14 years (*Druffel and Griffin*, 1999). The error range for the calibrated calendar age is reported as 1σ (95.4 statistical range). The calendar ages are reported as ka BP.

Appendix C

The International Equation of State for Seawater, 1980, UNESCO

The International Equation of State of Seawater is a mathematical expression adopted by the UNESCO, ICES, IAPSO Joint Panel on Oceanographic Tables and Standards to calculate the density of sea water (ρ, kg/m^3) as a function of practical salinity (S), temperature (t, °C) and applied pressure (p, bar) or other parameters derived from these.

In oceanography the term potential density (σ_θ = ρ - 1000) is commonly used. The potential density is the density at one atmosphere pressure ($p = 0$). Potential density can be computed from the practical salinity and the temperature with the following equation:

$$\begin{aligned}(\sigma_\theta) - 1000 &= p_w + [8.24493 * 10^1 - 4.0899 * 10^{-3} t + \\ &\quad 7.6438 * 10^{-5}(t^2) - 8.2467 * 10^{-7}(t^3) + \\ &\quad 5.3875 * 10^{-9}(t^4)]S + (-5.72466 * 10^{-3} + \\ &\quad 1.0227 * 10^{-4} t - 1.6546 * 10^{-6}(t^2))S^{3/2} + \\ &\quad 4.8314 * 10^{-4}(S^2)\end{aligned}$$

where p_w, the density of the Standard Mean Ocean Water (SMOW) taken as pure water reference is given by:

$$\begin{aligned}p_w &= 999.842594 + 6.793952 * 10^{-2} t - 9.095290 * 10^{-3}(t^2) + \\ &\quad 1.001685 * 10^{-4}(t^3) - 1.120083 * 10^{-6}(t^4) + 6.536332 * 10^{-9}(t^5)\end{aligned}$$

The Equation of State for Seawater Calculator can also be found on the web: http://ioc.unesco.org/oceanteacher/resourcekit/M3/Converters/- SeaWaterEquationOfState/Sea%20Water%20Equation%20of%20State%20Calculator.htm

Appendix D

Oxygen Solubility in Seawater

To determine the Apparent Oxygen Utilisation (AOU = $O_{2saturation}$ - $O_{2measured}$) in seawater we need to know the oxygen solubility (C^*_O) of seawater for a specific temperature and pressure. These equations of *Garcia and Gordon* (1992) use the experimental data from *Carpenter* (1966), *Murray and Riley* (1969) and *Benson and Krause* (1984) to improve on the original formulas by *Weiss* (1970) and *Chen* (1981) which do not fit the data very well below 1°C, or at high salinities.

Using a least squared method, a high precision formulae for estimating C^*_O has been developed, which behaves well at all extremes as well as the oceanic ranges of temperature and salinity(0≤t≤40°C and 0≤S≤42 ‰).

$$\begin{aligned} T_s &= ln[(298.15 - t)(273.15 + t)^{-1}] \\ lnC^*_O &= A_0 + A_1T_s + A_2T_s^2 + A_3T_s^3 + A_4T_s^4 + A_5T_s^5 + \\ &\quad S(B_0 + B_1T_s + B_2T_s^2 + B_3T_s^3) + C_OS^2 \end{aligned}$$

Where:

$$\begin{aligned} A_0 &= 5.80818 \\ A_1 &= 3.20684 \\ A_2 &= 4.11890 \\ A_3 &= 4.93845 \\ A_4 &= 1.015667 \\ A_5 &= 1.41574 \\ B_0 &= -7.01211 * 10^{-3} \\ B_1 &= -7.25958 * 10^{-3} \\ B_2 &= -7.9334 * 10^{-3} \\ B_3 &= -5.54491 * 10^{-3} \\ C_O &= -132412 * 10^{-7} \end{aligned}$$

Appendix E

Foraminifera

E.1 Planktic Foraminiferids

Planktic foraminiferids are unicellular organisms and are one of the most common groups of pelagic organisms in the open ocean today. Their global distribution, coupled with their prolific productivity and sensitivity to environmental parameters has led to their utilisation for interpreting ancient marine environments. Different species are found in a range of depths (Figure E.1) and habitats with varying interactions between biological factors (algal symbionts, nutrients, predation etc.) and physico-chemical factors (temperature, light, salinity, nutrients, water density, turbidity) (*Bé and Hutson*, 1977; *Bé*, 1977).

In this thesis stable isotopes from a suite of foraminiferal species with differing life cycles and ecology, which inhabit different water masses, have been used to highlight changes in ocean circulation at different water depths. Without water column studies, it is impossible to know the exact depth range of each species within this region. However, laboratory culturing (*Bijma et al.*, 1990; *Spero et al.*, 2003), and information from other regions provide us with general characteristic light, temperature and nutrient tolerances, life habitats and vital effects for different species.

E.1.1 *Globigerinoides ruber* (d'Orbigny, 1839)

Globigerinoides ruber is restricted to the upper 50 m of the water column as it is a spinose symbiotic foraminifera with large numbers of dinoflagellates in its protoplasm (*Bé and Hutson*, 1977). Although *G. ruber* may migrate below the surface mixed layer, it calcifies most of its test within the mixed layer and therefore records isotopic values of near surface waters. Sediment trap experiments and analysis of $\delta^{18}O$ from *G. ruber* tests have shown that the temperature of calcification agrees with temperatures at 3-4m below the surface (*Russell and Spero*, 2000). *G. ruber* has a life cycle of two weeks, and is present throughout the year in near constant numbers in strongly thermally stratified regions (*Deuser*, 1987; *Thunell and Reynolds*, 1984). It is found naturally within waters of 21 - 29°C and 34.5 - 36 ‰ salinity, although it appears to tolerate ranges of 16 - 31°C and 22 - 49 ‰ in the laboratory (*Bijma et al.*, 1990).

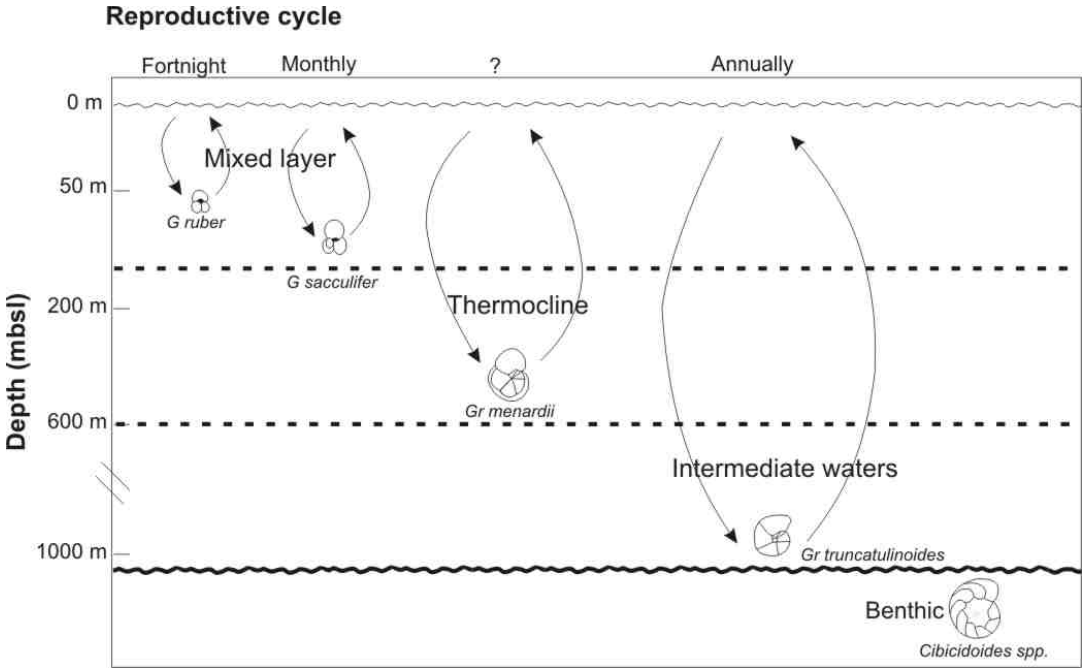

Figure E.1: Vertical distribution of the suite of foraminifera used in this thesis. From left to right with increasing depth range; planktonic species *Globigerinoides ruber*, *Globigerinoides sacculifer*, *Globoratalia menardii*, *Globoratalia truncatulinoides* and the Benthic family *Cibicdoides sp.* Reproduction cycles play an important part in the vertical distribution of the foraminifera within the water column (adapted from *Hemleben et al.* (1989).

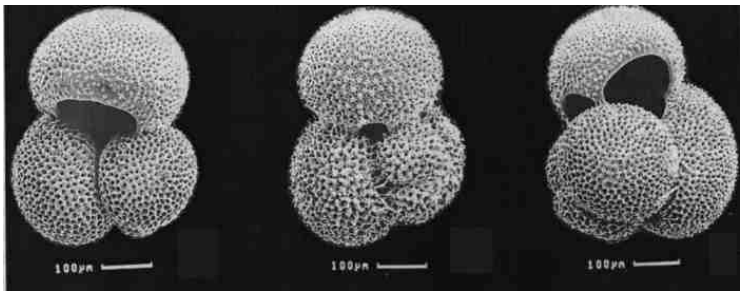

Figure E.2: *Globigerinoides ruber.*

Estimates of oxygen isotope vital effects for *G. ruber* vary widely with values varying from -0.2 ‰ (*Deuser*, 1987), -0.5 ‰ (*Fairbanks et al.*, 1982) and -0.6 ‰ (*Duplessy et al.*, 1981). There is no accepted value at present and hence it is rarely corrected for. Experimental work by *Spero et al.* (1997) has shown that significant variations in $\delta^{13}C$ and $\delta^{18}O$ can also be caused, by the Carbonate Ion Effect (CIE), whereby increasing $[CO_3^{2-}]$ results in a decrease of $\delta^{13}C$ and $\delta^{18}O$ within the test:

$$\begin{aligned} \delta^{13}C/[CO_3^{2-}] &= -0.0089 \pm 0.001 \ \mu mol^{-1}kg^{-1} \\ \delta^{18}O/[CO_3^{2-}] &= -0.0022 \pm 0.001 \ \mu mol^{-1}kg^{-1} \end{aligned}$$

The CIE, along with temperature, and test size all contribute to variations between the $\delta^{13}C$ of *G. ruber* and the $\delta^{13}C$ of TIC along a transect at 140°W in the Pacific (*Russell and Spero*, 2000).

G. ruber is solution susceptible, which affects the preservation and geochemical signature of individuals found at depth as the smaller juvenile individuals are preferentially dissolved. This depends on the chemistry of the bottom water (the calcite lysocline and CCD) and varies spatially as well as temporally. These variations must be accounted for when looking at the stable isotopes and geochemical tracers of *G. ruber* in different cores.

In the Indo Pacific region, the pink variety of *G. ruber* became extinct during the late Pleistocene at 120 kyr (*Thompson et al.*, 1979). As such , its last occurrence can be used as a chronostratigraphic marker in sedimentary marine cores. The pink variety is still present in the Atlantic and Mediterranean Sea.

Recent work by *Wang* (2000) in the South China Sea suggested that there are two morphotypes of *G. ruber* (white), which can be differentiated by their taxonomic and stable isotope compositions. *G. ruber s.s. (senso stricto)* (Figure E.2) lives in the upper 30 m of the water column, and *G. ruber s.l. (senso lato)* lives below 30 m. Evidence from sediment cores suggests that during MIS 2 there was very little difference between the stable isotopes of the morphotypes, possibly due to greater mixing (*Wang*, 2000). However this work has not been repeated. *G. ruber s.s* have been primarily been used in this study.

E.1.2 *Globigerinoides sacculifer* (Brady, 1877)

Globigerinoides sacculifer, also known as *G. quadrilobatus*, is the most common species in tropical to subtropical waters. Like *G. ruber*, it is photosymbiotic, live predominantly in the mixed layer the water column (*Nürnberg et al.*, 2000). It prefers to inhabit well-mixed, low seasonality waters with temperature >24°C and low vertical temperature gradients (*Thunell and Reynolds*, 1984). It also withstands a wide range of salinities: 24 - 47 ‰ and temperatures: 14-31°C, and is most abundant in low nutrient oligotrophic environments (*Bijma et al.*, 1990) feeding predominantly on calanoid copepods (*Hemleben et al.*, 1989).

Reproduction is linked to the lunar cycle. To reproduce, *G. sacculifer* undergoes gametogenesis when it sinks down through the water column to 80-100m depth and produces

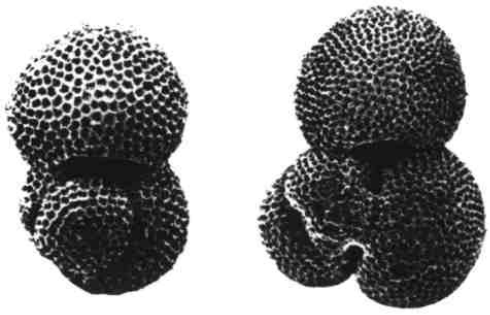

Figure E.3: *Globigerinoides quadrilobatus quadrilobatus (sacculifer).* Umbilical view (left), spiral view (right).

a secondary layer of calcite and also a fourth sac-like chamber. As gametogenic calcite is secreted in sea water of a different temperature and chemistry, tests with this gametogenic chamber are not included in any geochemical analyses.

G. sacculifer also shows changes in the stable isotope ratios as a result of the CIE (*Spero et al.*, 1997).

$$\begin{aligned} \delta^{13}C/[CO_3^{2-}] &= -0.0047 \pm 0.001 \ \mu mol^{-1} kg^{-1} \\ \delta^{18}O/[CO_3^{2-}] &= -0.0014 \pm 0.001 \ \mu mol^{-1} kg^{-1} \end{aligned}$$

Thus, for both isotope systems the effect on *G. sacculifer* is approximately half that for *G. ruber*. *G. sacculifer* is also thought to be closer in equilibrium to sea water chemistry as a result of reduced vital effects. So although it inhabits a wider depth range it may be a more reliable proxy for chemical and physical conditions within the mixed layer.

G. quadrilobatus quadrilobatus is differentiated from *G. quadrilobatus sacculifer* by workers who primarily work within the Holocene. The difference is that the *G. quadrilobatus quadrilobatus* does not produce a 4th gametogenic sac on its test. Workers studying foraminifera in the Quaternary have generally stuck with the name *G. sacculifer* for both species. Therefore, *G. quadrilobatus quadrilobatus* has primarily been picked for analyses, but continuing in the tradition of previous Quaternary workers, the label *G. sacculifer* has typically been used.

E.1.3 *Globoratalia menardii* (Parker, Jones and Brady, 1865)

Globorotalia menardii is a non-spinose planktonic species and, like all species of *Globorotalia*, exhibits a considerable vertical distribution throughout its life cycle. The foraminiferal test is dominated by two processes of growth: the accretion of chambers, and the formation of an enveloping calcite crust (*Schweitzer and Lohmann*, 1991). In the early stages, it lives in the euphotic zone in the upper 50 m of the water column. Measured isotopic compositions of whole specimens also indicates that this is where *Gr. menardii* secretes its main test. *Gr. menardii* then descend to the meso or bathypelagic depths in late ontogeny and the crust is emplaced at depths of between 50 and 200 m.

Figure E.4: *Globoratalia menardii*

Gr. menardii is a tropical species abundant at 20 to 25°C and ∼35 ‰ salinity (*Bé and Hutson*, 1977). It appears to increase in abundance in upwelling tropical waters and is common in shallow thermocline waters where primary productivity is high (*Thunell and Reynolds*, 1984; *Martinez et al.*, 1998; *Andreasen and Ravelo*, 1997). *G. menardii* abundance is closely coupled to the depth of the chlorophyll maximum (*Watkins et al.*, 1998).

E.1.4 *Globoratalia truncatulinoides*, (d'Orbigny 1839)

Globorotalia truncatulinoides (Figure E.5) is the deepest dwelling planktonic foraminifera used in this study. Although it appears in the upper few hundred metres of the water column it spends the majority of its life cycle below 100 m, calcifying the majority of its test at the base of the thermocline (*Fairbanks and Wiebe*, 1980; *Mulitza et al.*, 1997). It then appears to add its final calcite crust when it reaches the 10°C isotherm corresponding approximately to 1000 mbsl (*Hemleben et al.*, 1985). *Lohmann and Schweitzer* (1990) noted a correlation between the size and abundance of *Gr. truncatulinoides* and the depth of the thermocline, and suggested that vertical mixing down to 600 mbsl was required for the species to complete its annual reproductive cycle.

Recent work studying the morphological and DNA of *Gr. truncatulinoides* has shown that there are four distinct genotypes formed by adaptive radiation at around 500kyr, which inhabit different ecological niches. Species 1 and 2 characterize subtropical waters, Species 3 is abundant and exclusively found at the Subantarctic front, and Species 4 inhabits the cold, nutrient rich Subantarctic waters (*de Vargas et al.*, 2001). It is likely that both Sp. 1 and 2 exist in the Tasman Sea. The two species can be distinguished on coiling directions with left coiling Sp. 1 inhabiting low nutrient, distal sites, whilst Sp. 2 is mainly dextral and inhabits the margins of subtropical gyres where coastal upwelling and seasonal phytoplankton blooms occur. The majority of the *Gr. truncatulinoides* in this study were right coiling and therefore, we conclude that Sp. 2 dominates this region when suitable conditions prevail.

Figure E.5: *Globoratalia truncatulinoides*

E.2 Benthic Foraminiferids

Benthic foraminiferids are found living at or near the sediment/water interface. They are primarily influenced by environmental factors such as organic content (food supply). Recent work suggests that oxygen content of the bottom waters has little influence in controlling faunal distributions (*Rathburn and Corliss*, 1994). Variations in microhabitats influence the stable isotope of the calcite shell produced by different species (*Rathburn et al.*, 1996).

E.2.1 *Cibicidoides sp.* (Phleger and Parker 1951)

Due to the relatively minor abundance of benthic foraminifera within the cores, several species from *Cibicidoides* family were combined to obtain sufficient numbers of individuals and mass for stable isotope analyses. Froom the literature many of the species are known by a range of names determined by their age, size and location. The family is also often called *Cibicides*.

The main species used were

- *C. psuedoungeriana* (Cushman 1931) (Figure E.6) this is also commonly known as *C. pachyderma* (Rzehak 1886) and *C. floridanus* (Cushman 1951) and many other synonyms are suspected. It is primarily a Neogene taxa but ranges from Oligocene through to Holocene. Usually it inhabits the upper bathyal depths, although it has been found in shelf assemblages and at paleodepths of 3615m (*Berggren et al.*, 1976).

- *C. kullenbergi* (Parker 1953) (Figure E.7) This is also known as *C. mundulus* (Brady, Parker and Jones 1888), the main difference being the test size and therefore *C. kullenbergi* is considered to be a junior synonym of *C. mundulus*. It also ranges from Oligocene through to Holocene. It is considered a bathyal to abyssal species. *Corliss* (1985) observed *C. kullenbergi* as infaunal living within the tope 0-2 cm of the sediment. *Boersma* (1986) recorded their presence within the Coral and Tasman seas.

- *C. wuellerstorfi* (Schwager 1866) (Figure E.8)This is also assigned to the families *Anomalina, Planulina* and *Truncatalina*. It is a well known, truly cosmopolitan

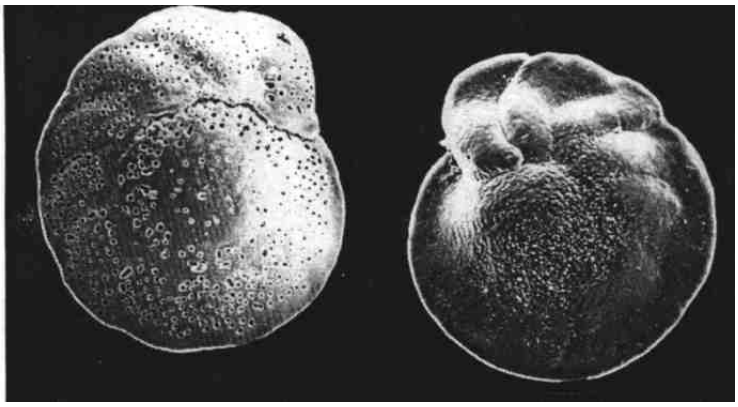

Figure E.6: *Cibicidoides pseudoungeriana*

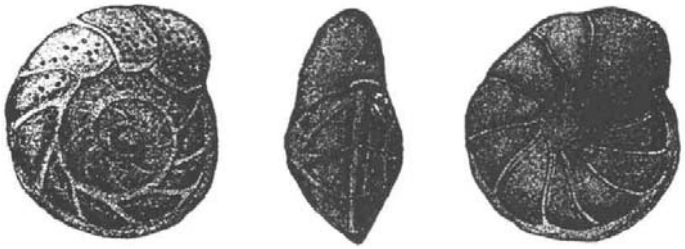

Figure E.7: *Cibicidoides kullenbergi*

Figure E.8: *Cibicidoides wuellerstorfi*

deep water taxa ranging from the Middle Miocene through the Holocene. It is a lower bathyal and abyssal species and is rare between 500 m and 3000 m. It appears its abundance maxima is reached at depths of >3000 mbsl.

The *Cibicidoides* genera are predominantly epifaunal benthics with similar micro habitats. The carbon isotopic composition of benthic species varies according to microhabitat preferences and pore water chemistry. The three species described above show similar offsets within the accuracy of the method and are closely enough related in habitat and

biological influences to give similar stable isotope values. So for this study *Cibicidoides* specimens were only picked down to genus level (an approach used by many others) (*McCorkle et al.*, 1990; *Shackleton and Hall*, 1997; *Woodruff et al.*, 1980) The exception to this rule is *C. bradyi*, which has a different microhabitat preference (*Rathburn et al.*, 1996). Therefore, *C. bradyi* was not picked for stable isotope analysis. Due to the epifaunal nature of *Cibicidoides* the $\delta^{13}C$ of the genus is considered to reflect the $\delta^{13}C$ of bottom water with relatively little fractionation (*McCorkle et al.*, 1990; *Zahn et al.*, 1986)

Oxygen isotopes of benthic foraminifera show no relationship to microhabitat preference (*Rathburn and DeDeckker*, 1997). However, vital effects produce a regular $\delta^{18}O$ offset from the surrounding water. These are usually corrected for using various adjustment factors (*Shackleton and Hall*, 1997). The adjustment factors used for *Cibicidoides sp.* is +0.5-0.64‰ (*Shackleton and Hall*, 1997). In this study, the $\delta^{18}O$ values have been corrected by +0.64‰.

Appendix F

Wind Stress Curl and EAC Circulation

Written with the help of Andrew Kiss.

The following equations describe the relationship between the surface winds and the ocean currents.

F.1 Surface Winds

Let x and y signify east-west and north-south, and denote the wind stress vector by $\tau = (\tau_x, \tau_y)$, where τ_x and τ_y are the eastward and northward components of the stress (the stress τ is in the direction of the surface winds).

The curl of the wind stress is defined as

$$curl\tau = \frac{\partial \tau_y}{\partial x} - \frac{\partial \tau_x}{\partial y},$$

where ∂ denotes a partial derivative, eg. $\partial\tau_x/\partial y$ is the gradient of the zonal wind stress τ_x as a function of latitude y.

Consider τ to be due to a zonally averaged wind; since it is therefore independent of longitude x we have curl τ = - $\partial\tau_x/\partial y$.

F.2 Ocean currents

Let u and v be the eastward and northward velocity components of the horizontal depth-averaged ocean flow. At the scale of an ocean basin the time-averaged flow is governed by the *Sverdrup* (1947) relation, which states that

$$v = Kcurl\tau = -K\frac{\partial \tau_x}{\partial y},$$

where K is a positive constant. Thus the north-south velocity is proportional to the north-south variation in the zonal wind, and we can therefore have meridional flow driven by

purely zonal wind. In the subtropics in the Southern Hemisphere curl τ is positive due to the subtropical westerlies (τ_x >0) changing to easterly trade winds (τ_x <0) as y increases to the north; this produces a northward Sverdrup flow ($v > 0$).

The eastward velocity u can be determined from the requirement that meridional gradient in v be compensated by zonal gradient in u so that mass is conserved. This is expressed mathematically as

$$\frac{\partial u}{\partial x} = \frac{-\partial v}{\partial y} = K\frac{\partial^2 t_x}{\partial y^2},$$

where the last step follows from the Sverdrup relation. Integrating this expression westwards from the eastern boundary x_E (where $u = 0$) yields

$$u = K(x - x_E)(\frac{\partial^2 t_x}{\partial y^2}),$$

So, the eastward velocity is proportional to both the distance from the eastern boundary and the second meridional derivative of the zonal wind stress (or equivalently, the meridional gradient in the wind stress curl). Note the eastward flow u is not simply driven by the eastward wind stress τ_x as we might intuitively assume, but by details of its meridional variation; in some circumstances u can actually be in the opposite direction to τ_x. These equations give the components u and v of the "Sverdrup flow" which occurs in the whole basin, except the WBC. This large-scale flow forms a recirculating gyre with northern and southern boundaries given by latitudes of purely zonal flow, which occurs where

$$v = Kcurl\tau = 0.$$

Between these latitudes there is a net Sverdrup transport (northwards in the Southern Hemisphere subtropics) which is compensated by a much narrower (and therefore much more rapid) return flow along the western boundary - this is the dynamical origin of the southward East Australian Current (EAC).

Appendix G

Abbreviations

AABW	Antarctic Bottom Water
AAIW	Antarctic Intermediate Water
AASW	Antarctic Surface Water
ACC	Antarctic Circumpolar Current
Alk	Alkalinity
AMS	Accelerator Mass Spectrometer
ANU	Australian National University
BMR	Bureau of Mineral Resources
CCD	Carbonate Compensation Depth
CLIMAP	Climate: Long range Investigation, Mapping and Prediction
CPDW	Circumpolar Deep Water
CTD	Conductivity, temperature, depth profile
DSDP	Deep Sea Drilling Program
EAC	East Australian Current
EEP	Eastern Equatorial Pacific
ENSO	El Niño Southern Oscillation
EqIW	Equatorial Intermediate Waters
EUC	Equatorial Undercurrent
GBR	Great Barrier Reef
GEOSECS	Geochemical Oceans Sections Study
IPWP	Indo-Pacific Warm Pool
ITCZ	Inter Tropical Convergence Zone
JGOFS	Joint Global Ocean Flux Study
LGM	Last Glacial Maximum
mbsl	metres below sea level
MIS	Marine Isotope Stage
NADW	North Atlantic Deep Water
NEC	North Equatorial Current
NECC	North Equatorial Counter Current
NEqIW	Northern Equatorial Intermediate Water
NGCUC	New Guinea Coastal Undercurrent

NPIW	North Pacific Intermediate Water
ODP	Ocean Drilling Program
PDW	Pacific Deep Water
PF	Polar Front
PV	Potential Vorticity
SAF	Subantarctic Front
SAMW	Subantarctic Mode Water
SEC	South Equatorial Current
SEqIW	Southern Equatorial Intermediate Water
SMOW	Standard Mean Ocean Water
SPC	South Pacific Current
SPECMAP	Spectral Mapping Project
SSS	Sea Surface Salinity
SST	Sea Surface Temperature
STF	Subtropical Front or Subtropical Convergence (STC)
TF	Tasman Front
THC	Thermohaline Circulation TIC
T-O	potential Temperature v Oxygen
T-S	potential Temperature v Salinity
T-tracer	potential Temperature v geochemical tracer plot
WBC	Western Boundary Currents
WOCE	World Ocean Circulation Experiment
WSPCW	West South Pacific Central Waters